Journal of Robotics and Control (JRC)
Volume 4, Issue 1, January 2023
ISSN: 2715-5072, DOI: 10.18196/jrc.v4i1.16445

A Novel Improved Sea-Horse Optimizer for Tuning Parameter Power System Stabilizer

Widi Aribowo *
Department of Electrical Engineering, Universitas Negeri Surabaya, Surabaya, Indonesia
Email: widiaribowo@unesa.ac.id
*Corresponding Author

Abstract*— Power system stabilizer (PSS) is applied to dampen system oscillations so that the frequency does not deviate beyond tolerance. PSS parameter tuning is increasingly difficult when dealing with complex and nonlinear systems. This paper presents a novel hybrid algorithm developed from incorporating chaotic maps into the sea-horse optimizer. The algorithm developed is called the chaotic sea-horse optimizer (CSHO). The proposed method is adopted from the metaheuristic method, namely the sea-horse optimizer (SHO). The SHO is a method that duplicates the life of a sea-horse in the ocean when it moves, looks for prey and breeds. In This paper, The CSHO method is used to tune the power system stabilizer parameters on a single machine system. The proposed method validates the benchmark function and performance on a single machine system against transient response. Several metaheuristic methods are used as a comparison to determine the effectiveness and efficiency of the proposed method. From the research, it was found that the application of the logistics Tent map from the chaotic map showed optimal performance. In addition, the application of the PSS shows effective and efficient performance in reducing overshoot in transient conditions.

***Keywords*— Smib; Chaotic sea-horse optimizer; Metaheuristic; Power system stabilizer; Power system.**

I. INTRODUCTION

Rapid technological developments indirectly affect the stability and efficiency of the power system [1]–[4]. Low frequency oscillations are a big challenge in power systems [5]–[10] . This affects the toughness of the system as a single machine or interconnection if it cannot be responded to appropriately [11]–[15]. Inappropriate response will affect the electricity supply which results in economic losses. Tremendous negative effect on system stability caused by low frequency oscillations so that maximum effort is required. The stability of the power system is a key word that must always be maintained [16]–[21].

Power System Stabilizers (PSS) are a well-known and effective approach to dealing with low frequency oscillations [22]–[27]. PSS is applied to maintain the stability of the power system either as a single machine or interconnection [28]–[33]. PSS is designed with the nature of the system in mind. The non-linear characteristics of the power system and consistent fluctuations over a wide range can make conventional PSS insufficient to achieve optimal performance. In addition, conventional PSS has approaches such as self-tuning regulators and feedback linearization. However, this approach presents drawbacks such as intensive computing and long computer processing times [34]–[36]. To overcome these problems and produce more efficient and optimal solutions. Several algorithmic approaches have been presented by researchers as alternative methods.

The development of computing technology indirectly encourages the development of several new algorithms. There has been a significant increase from the discovery of new metaheuristic methods in recent years to get better optimizations for non-linear and complex problems. The application of traditional deterministic optimization methods often encounters several problems such as balance in exploitation-exploration, deadlock with local optimization and cannot be separated from derivatives. Metaheuristic algorithm has the characteristics of a simple, and optimal approach. In addition, metaheuristic algorithms are also durable and self-organized. Some of the latest metaheuristic algorithms in recent years such As FOX [37], Giant Trevally Optimizer [38], Dung beetle optimizer [39], Ebola optimization search algorithm [40], Dwarf mongoose optimization algorithm [41], Snake Optimizer [42]. Arithmetic Optimization Algorithm [43], Archimedes Optimization Algorithm [44], Remora Optimization Algorithm [45], African Vultures Optimization Algorithm [46], Horse Herd Optimization Algorithm [47], Battle Royale Optimization Algorithm [48], Chimp Optimization Algorithm [49], Pelican Optimization Algorithm [50], Prairie Dog Optimization Algorithm [51], and Group Search Optimizer [52]. The average output of the applied method produces the optimal approach for a particular solution.

The application of metaheuristic methods in adjusting the power system stabilizer has provided promising performance. Several metaheuristic algorithms have been applied to power system stabilizers in recent years, such as Atomic Search Optimization [53], Ant Colony Optimization Algorithm [54], [55], Crow Search Algorithm [56], Tunicate Swarm Algorithm [57], Harris Hawk Optimizer [58], [59], Moth Search Algorithm [60], [61], Mayfly Optimization Algorithm [62], Sine-Cosine Algorithm [63], Rat Swarm Optimization [64], Whale Optimization Algorithm [65], [66] and Particle Swarm Optimization [67]–[70]

Several researchers have also presented a combination of metaheuristic algorithms for tuning PSS parameters, such as Gude et al demonstrated a combination of butterfly optimization algorithm and particle swarm optimization [71]. Kalegowda et al presented a combination of Particle swarm optimization and Taguchi algorithm [72]. Devarapalli et al presented a combination of gray wolf optimization, sine cosine algorithm and cuckoo search [73]. Penchalaiah et al presented a combination of Harris Hawks Optimization Algorithm and the Tabu Search Algorithm [74]. Although several metaheuristic algorithms have been demonstrated for PSS tuning, there is still a lot of room to be explored to get an optimal PSS performance. Therefore, this study presents a PSS parameter tuning approach with the latest metaheuristic algorithm called Sea-Horse Optimizer (SHO) which is improved by adding a chaotic algorithm [75]. This hybrid method is called the Chaotic Sea-Horse Optimizer (CSHO) method which aims to improve the performance of the SHO algorithm at the center of the balance between exploration and exploitation. The proposed method is an integration of chaotic and SHO methods. The contribution of this research can be briefly described as follows:

1. A hybrid algorithm is presented, namely Chaotic Sea-Horse Optimization (CSHO) which has a new balance between exploration and exploitation phases.
2. The proposed CSHO is applied to tune the power system stabilizer parameters.

This article consists of several sessions, namely: Part 2 explains the Sea-Horse Optimizer method, the novel Chaotic Sea-Horse Optimizer and power system stabilizers. Session 3 contains the design of the proposed control. The simulation results and discussion are presented in session 4. The last session contains conclusions and future works.

II. METHODS

A. Sea-Horse Optimizer (SHO)

The sea-horse optimizer (SHO) is inspired by the life of seahorses while searching for prey, movement and breeding in the sea. The concept of exploration and exploitation that characterizes the metaheuristic method in the SHO algorithm is designed to adopt the social behavior of movement and search for seahorse prey. The last phase of breeding is executed when the two components have ended. The SHO method can be modeled in detail as follows:

$$Sh = \begin{bmatrix} x_{1,i} & \cdots & x_{1,Dim-1} & x_{1,Dim} \\ x_{2,i} & \cdots & \cdots & x_{2,dim} \\ \vdots & \vdots & \vdots & \vdots \\ x_{N,i} & \cdots & x_{N,Dim-1} & x_{N,Dim} \end{bmatrix} \quad (1)$$

$$Sh_{ij} = Rand \times (UB_j - LB_j) + LB_j \quad (2)$$

$$Sh_{elite} = argmin(f(X_i)) \quad (3)$$

Where Dim is the dimension of the variable and N is size of population. The upper and lower limits are symbolized by UB and LB which are random results from each solution. Random value with a range from 0 to 1 is denoted by $Rand$. Sh_{elite} is a symbol of individuals who have a minimum level of fitness represented as elite individuals. SHO adopts the life of seahorses in the form of movement, looking for prey and breeding.

Seahorse Movement Behavior

The normal distribution becomes a reference in the movement pattern of seahorses. balance of exploration and exploitation using two case studies with a boundary point of 0.

Case 1: the agent moves towards the X_{elite} in a spiral motion and changes the rotation angle constantly to widen the local solution region. Case 1 can be formulated mathematically as follows:

$$X_n(t+1) = X_i(t) + Levy(\lambda)((X_{elite}(t) - X_i(t)) \times x \times y \times z + X_{elite}(t)) \quad (4)$$

$$\theta = rand \times 2\pi \quad (5)$$

$$x = \times \cos(\theta) \quad (6)$$

$$y = \rho \times \sin(\theta) \quad (7)$$

$$z = \rho \times \theta \quad (8)$$

$$\rho = \mu \times e^{\theta v} \quad (9)$$

$$Levy(\lambda) = s \times \frac{w \times \sigma}{|K|^{\frac{1}{\lambda}}} \quad (10)$$

$$\sigma = \left(\frac{\Gamma(1+\lambda) \times \sin\left(\frac{\pi \lambda}{2}\right)}{\Gamma\left(\frac{1+\lambda}{2}\right) \times \lambda \times 2^{\left(\frac{\lambda-1}{2}\right)}} \right) \quad (11)$$

Where the length of the rod specified by the logarithmic spiral constant u (default=0.05) and v (default=0.05) is denoted by ρ. λ is a random number [0, 2]. k and w are random numbers [0, 1]. s is a fixed constant of 0.01.

Case 2: with ocean waves, the seahorse performs a brownian motion that mimics the motion length of another seahorse in an attempt to get a better traverse. This can be formulated as follows:

$$X_n(t+1) = X_i(t) + rand \times l \times \beta_i \times (X_i(t) - \beta_i \times X_{elite}(t)) \quad (12)$$

$$\beta_i = \frac{1}{\sqrt{2\pi}} \exp\left(-\frac{x^2}{2}\right) \quad (13)$$

$$X_n(t+1) = \begin{cases} X_i(t) + Levy(\lambda)((X_{elite}(t) - X_i(t)) \times x \times y \times z + X_{elite}(t)) & if\ r_1 > 0 \\ X_n(t+1) = X_i(t) + rand \times l \times \beta_i \times (X_i(t) - \beta_i \times X_{elite}(t)) & if\ r_1 \le 0 \end{cases} \quad (14)$$

where β_i is the random walk coefficient of the brownian motion. l is a constant value (default=0.5). r_1 is symbolized as a random value

Seahorse Foraging Behavior

When seahorses look for food there are 2 possible outcomes, namely success and failure. The condition is successfully set with a value of $r_2 > 0.1$. This condition when the seahorse moves faster than the prey. On the other hand, a failure condition occurs when the response is different. The conditions of failure and success of seahorses when looking for food can be formulated as follows:

$$X_n(t+1) = \begin{cases} \alpha \times ((X_{elite}(t) - rand \times X_{new}(t)) + (1-\alpha) \times X_{elite}(t)) & if\ r_2 > 0 \\ (1-\alpha) \times ((X_{new}(t) - rand \times X_{elite}(t)) + (\alpha) \times X_{new}(t)) & if\ r_2 \le 0 \end{cases} \quad (15)$$

$$\alpha = (1 - \frac{t}{T})^{\frac{2t}{T}} \tag{16}$$

where X_{new} new is the new position of the seahorse. r_2 is a random number [0, 1]. T is the maximum iteration.

Seahorse Breeding Behavior

At the time of breeding, seahorses are divided into 2 sex groups, namely male and female with the same amount of composition, namely 50%

$$Father = X_{sort}\ (1{:}\frac{pop}{2}) \tag{17}$$

$$Mother = X_{sort}\ (\frac{pop}{2} + 1 : pop) \tag{18}$$

Sorted X_{sort} values return the result in ascending order. $Father$ and $Mother$ were chosen randomly. In the SHO algorithm, each pair produces one child.

$$X_i = (1 - r_3)X_{mother} + r_3 X_{father} \tag{19}$$

Where r_3 is a random number [0, 1].

B. The Novel Chaotic Sea-Horse Optimizer (CSHO)

Several articles have used several types of chaotic maps for the purpose of algorithm optimization. Chaotic maps are dynamic in character and statistics built on randomness [76], [77]. Future or future behavior is affected by parameter changes. So that small changes to the parameters produce different outputs. In this article, the logistic type chaotic map is used to replace the $rand$ in Equation (5). The mathematical equation of the logistic type chaotic map is as follows:

$$ylog_{(i+1)} = a \times ylog_{(i)}\left(1 - ylog_{(i)}\right) \tag{20}$$

Where a is 4. So, the chaotic map variable with range [0, 1] is obtained. So, Equation (5) turns into Equation (21) as follows:

$$\theta = ylog \times 2\pi \tag{21}$$

Pseudo code from CSHO can be seen in Algorithm 1.

Algorithm 1 Pseudo Code of Chaotic Sea-Horse Optimizer

Input: population size pop, maximum iteration T and variable dimension Dim
Output: Optimal search agent Xbest
1: **procedure CSHO**
2: Initialize search agent Xi
3: Calculate the fitness value of each search agent
4: Determine thes best search agent Xe
/* Movement behavior */
5: **While (t<Max_iteration) do**
6: **if r1 = randn > 0 do**
7: $u \leftarrow 0.05$
8: $v \leftarrow 0.05$
9: $l \leftarrow 0.05$
10: $ylog_{(i+1)} \leftarrow a \times ylog_{(i)}\left(1 - ylog_{(i)}\right)$ using Eq. (20)
11: $\theta \leftarrow ylog \times 2\pi$ using Eq. (21)
12: $x \leftarrow \cos(\theta)$ using Eq. (6)
13: $y \leftarrow \rho \times \sin(\theta)$ using Eq. (7)
14: $z \leftarrow \rho \times \theta$ by using Eq. (8)
15: $\rho \leftarrow \mu \times e^{\theta v}$ by using Eq. (9)
16: **else if do**
17: update positions of the search agent by using Eq. (12)
18: end if
/* Foraging behavior */
19: update positions of the search agent by using Eq. (15)
20: Calculate the fitness value of each search agent
/* Foraging behavior */
21: Select fathers and mother by using Eq. (17) and Eq. (18)
22: Breed Offsping by using Eq. (19)
23: Calculate the fitness value of each offspring
24: Select the next iteration population from the offspring and parent ranked top pop in fitness values
25: Update elite (X_{elite}) position
26: $t \leftarrow t + T$
27: **end while**
28: **end procedure**

C. Power System Stabilizer

The main function of PSS is to produce a suitable damping torque on the engine rotor. This aims to obtain compensation from the phase lag between the excitation input and the electric torque [78]–[80]. So that the PSS output is proportional to the rotor speed. The widely used conventional lead-lag PSS structure can be seen in Fig. 1

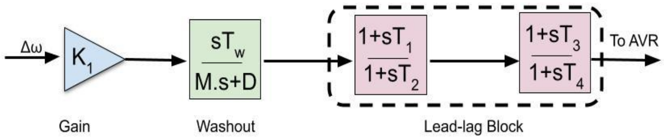

Fig. 1. PSS lead-lag type [81]

The optimal value of the PSS lead-lag parameter was optimized using CSHO. This is to improve the closed-loop response of the system to the terms of the transient response criteria. Fig. 2 illustrates the block diagram of the proposed CSHO-PSS approach.

III. DESIGN OF CONTROLLERS

The optimal value of the PSS lead-lag parameter was optimized using CSHO. This is to improve the closed-loop response of the system to the terms of the transient response criteria. Fig. 2 illustrates the block diagram of the proposed CSHO-PSS approach. some guidelines for getting PSS parameters with CSHO, namely:

- Step one: start by creating a single machine system
- Step two: design and build the CSHO algorithm
- Step three: Perform CSHO integration with single machine
- Step four: the system is run according to the desired constraints to get the PSS parameters
- Step five: Get the PSS parameters
- Step six: done

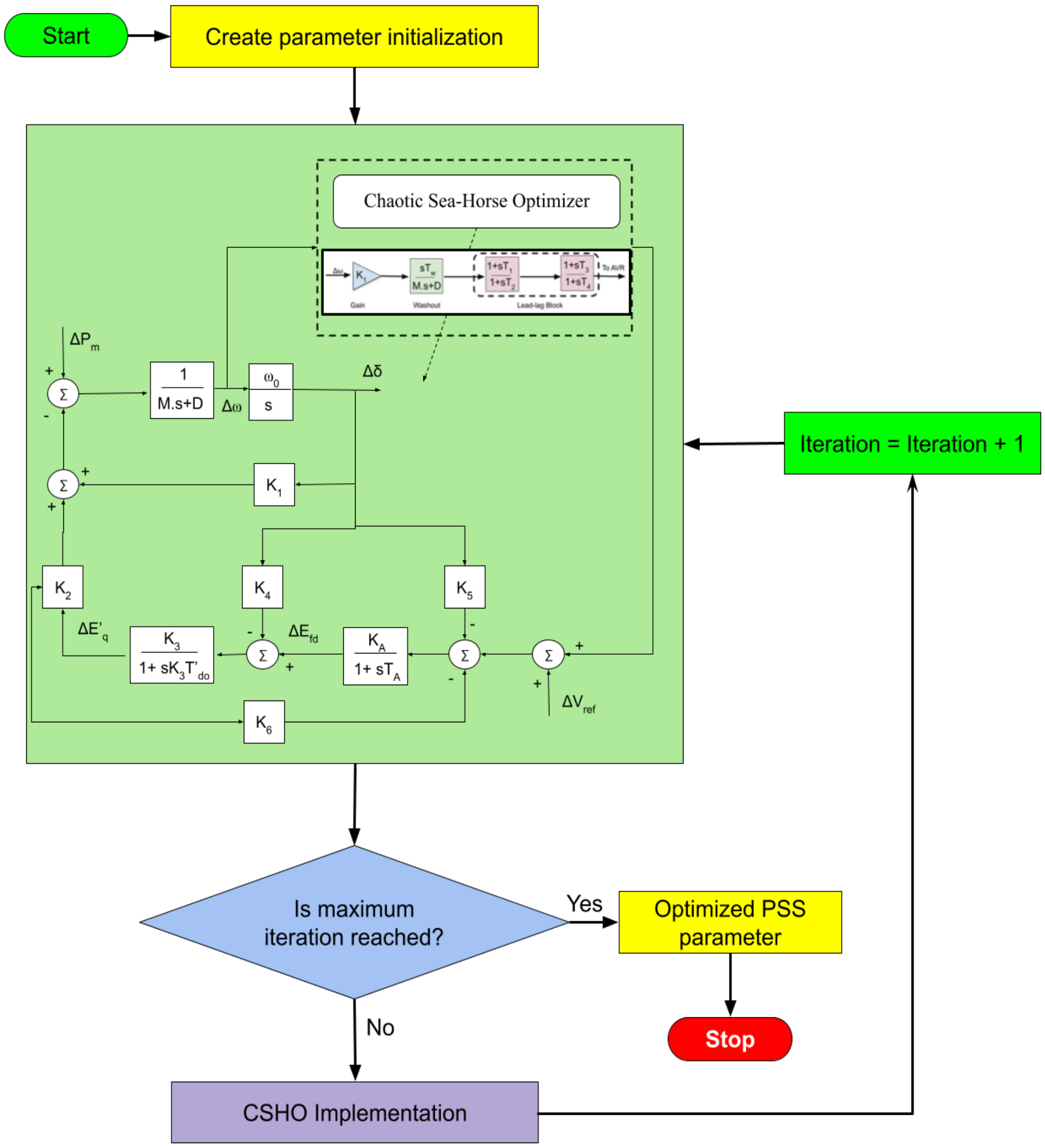

Fig. 2. Block diagram of the proposed CSHO algorithm implementation on PSS Lead-Lag.

TABLE I. UNIMODAL FUNCTION[82], [83]

Test Function	Range
$F_1(x)=\sum_{i=1}^{n} X_i^{\,2}$	$[-100,100]^n$
$F_2(x)=\sum_{i=1}^{n}\lvert X_i\rvert+\prod_{i=1}^{n}\lvert X_i\rvert$	$[-10,10]^n$
$F_3(x)=\sum_{i=1}^{n}(\sum_{j=1}^{n}\lvert X_i\rvert)^2$	$[-100,100]^n$
$F_4(x)=\max\{\lvert X_i\rvert, 1\le i\le n\}$	$[-100,100]^n$
$F_5(x)=\sum_{i=1}^{i_{n-1}}[100(x_{i+1}-x_1^{\,2})^2+(x_i-1)^2]$	$[-30,30]^n$
$F_6(x)=\sum_{i=1}^{n}(\lvert X_i+0.5\rvert)^2$	$[-100,100]^n$
$F_7(x)=\sum_{i=1}^{n} iX_i^{\,4}+random(0,1)$	$[-1.28,1.28]^n$

TABLE II. MULTIMODAL FUNCTION

Test Function	S
$F_8(x) = \sum_{i=1}^{n} -X_i \sin(\sqrt{\lvert X_i \rvert})$	$[-500,500]^n$
$F_9(x) = \sum_{i=1}^{n} [X_i^2 - 10\cos(2\pi X_i) + 10]$	$[-5.12,5.12]^n$
$F_{10}(x) = -20\exp(-0.2\sqrt{\frac{1}{n}\sum_{j=1}^{n} X_i^2}) - \exp(\frac{1}{n}\sum_{i=1}^{n}\cos(2\pi X_i)) + 20 + e$	$[-32,32]^n$
$F_{11}(x) = \frac{1}{4000}\sum_{i=1}^{n} X_i^2 + \prod_{i=1}^{n}\cos(\frac{X_i}{\sqrt{i}}) + 1$	$[-20,20]^n$
$F_{12}(x) = \frac{\pi}{n}\left\{10\sin(\pi y_1) + \sum_{i=1}^{n-1}(y_i-1)^2[1+10\,sin^2(\pi y_{i+1}) + (y_i-1)^2]\right\} + \sum_{i=1}^{n} u(x_i,10,100,4)$ $y_i = 1 + \frac{x_i+1}{4}$ $\mathrm{U}(x_i,a,k,m) = \begin{cases} k(x_i-a)^m & x_i > a \\ 0 & -a < x_i < a \\ k(-x_i-a)^m & x_i < -a \end{cases}$	$[-50,50]^n$
$F_{13}(x) = 0.1\{\{\sin^2(3\pi x_i) + \sum_{i=1}^{n}(X_i-1)^2[1+\sin^2(3\pi x_i+1)] + (X_i-1)^2[1+\sin^2(2\pi x_n)]\} + \sum_{i=1}^{n} u(X_i,5,100,4)$	$[-50,50]^n$

TABLE III. MULTIMODAL FUNCTION WITH FIX DIMENSION

Test Function	S
$F_{14}(x) = (\frac{1}{500} + \sum_{j=1}^{25}\frac{1}{j+\sum_{i=1}^{2}(x_i-a_{ij})^6})^{-1}$	$[-65.53,65.53]^2$
$F_{15}(x) = \sum_{j=1}^{11}\left[a_i - \frac{x_i(b_i^2+b_ix_2)}{b_i^2+b_ix_3+x_4}\right]^2$	$[-5,5]^4$
$F_{16}(x) = 4x_i^2 - 2.1x_1^4 + \frac{1}{3}x_1^6 + x_1x_2 - 4x_2^2 + 4x_2^4$	$[-5,5]^2$
$F_{17}(x) = \left(x_2 - \frac{5.1}{4\pi^2}x_1^2 + \frac{5}{\pi}x_1 - 6\right)^2 + 10\left(1-\frac{1}{8\pi}\right)\cos x_1 + 10$	$[-5,10]\times[0,15]$
$F_{18}(x) = [1+(x_1+x_2+1)^2(19-14x_1+3x_1^2-14x_2+6x_1x_2+3x_2^2)]\times[30+(2x_1-3x_2)^2\times(18-32x_1+12x_1^2+48x_2-36x_1x_2+27x_2^2)]$	$[-2,2]^2$
$F_{19}(x) = -\sum_{i=1}^{4} C_i\exp(-\sum_{i=1}^{3} a_{ij}(X_i-p_{ij})^2)$	$[0,1]^3$
$F_{20}(x) = -\sum_{i=1}^{4} C_i\exp(-\sum_{i=1}^{6} a_{ij}(X_i-p_{ij})^2)$	$[0,1]^6$
$F_{21}(x) = -\sum_{i=1}^{5}[(X-a_i)(X-a_i)^T + C_i]^{-1}$	$[0,10]^4$
$F_{22}(x) = -\sum_{i=1}^{7}[(X-a_i)(X-a_i)^T + C_i]^{-1}$	$[0,10]^4$
$F_{23}(x) = -\sum_{i=1}^{10}[(X-a_i)(X-a_i)^T + C_i]^{-1}$	$[0,10]^4$

IV. Simulation Result and Discussion

A. Convergence Profile

The performance measurement of the CSHO algorithm uses the benchmark function. Details of the benchmark functions used in this article can be seen in Table 1 to Table 3. Unimodal functions ranging from F1 to F7 can be seen in Table 1. While multimodal functions can be seen from F8 to F13 can be seen in Table 2. Functions F14 to F23 are multimodal functions with fixed dimensions can be seen in Table 3.

The MATLAB/Simulink software via a laptop with an Intel I5-5200 2.19 GHz processor and 8 GB RAM is used for programming algorithm codes, simulating transient response, and robustness. The parameters of the CSHO algorithm in detail are listed in Table IV.

The proposed CSHO algorithm uses a population size of 50 while the maximum iteration limit is set at 30. This study uses the GOA, WOA and SHO algorithms as comparisons. The results of the comparison with the benchmark function from F1 to F23 are presented in Fig. 3.

TABLE IV. Parameter CSHO

Parameter	Value
Number Of Sea-Horse (population)	50
u	0.05
v	0.05
l	0.05
a (*chaotic map parameter*	4
Maximum Iteration	30

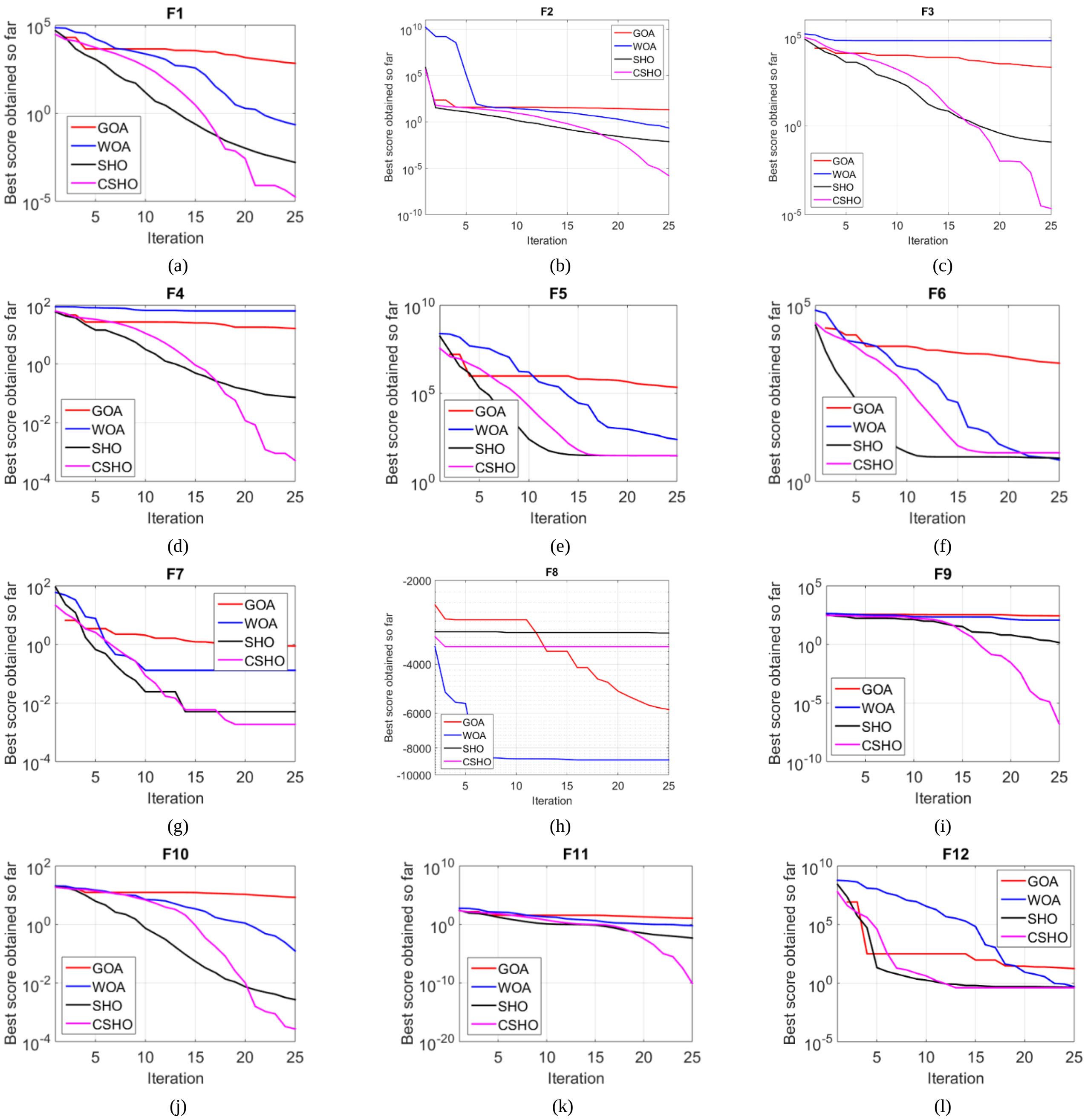

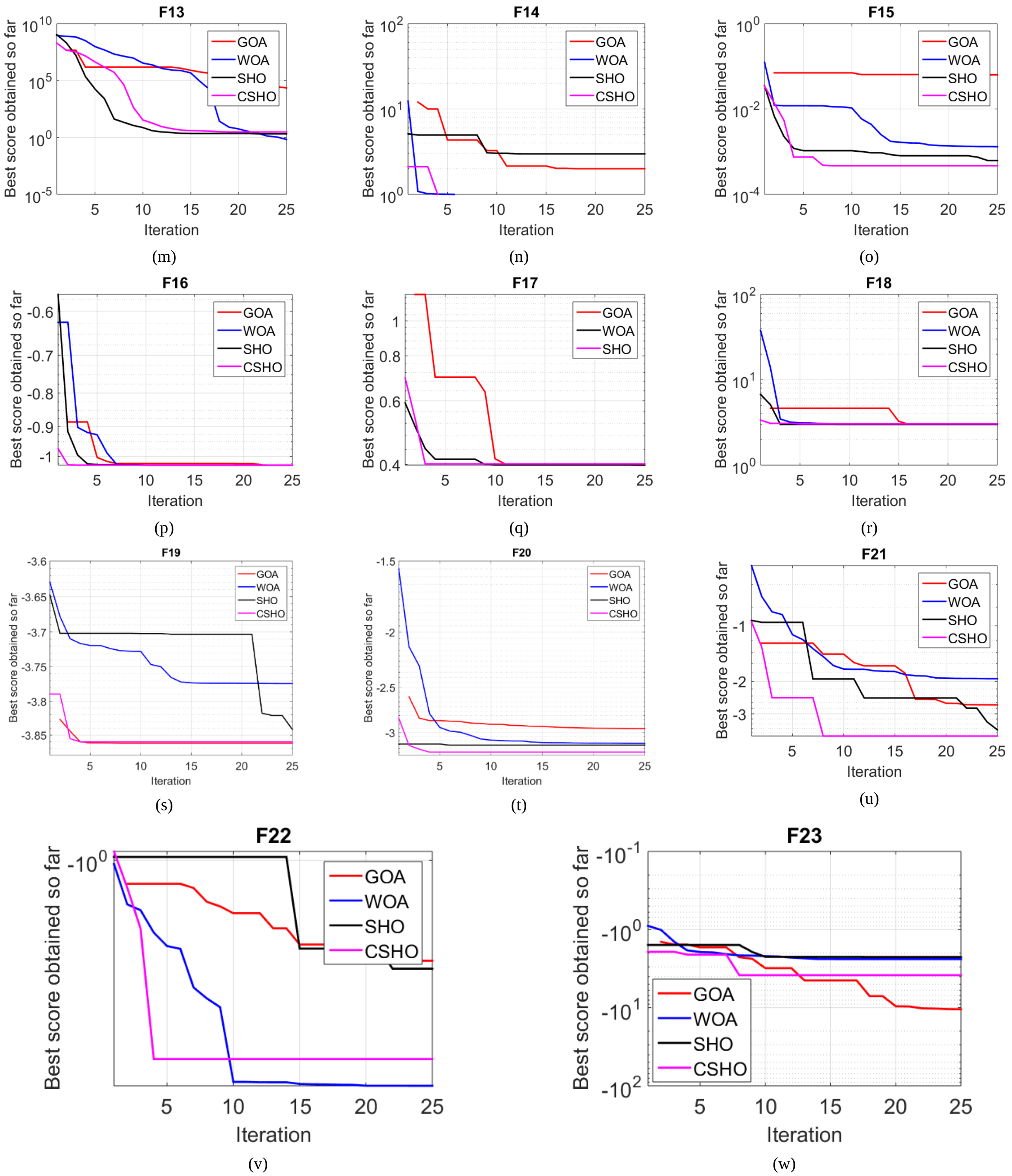

Fig. 3. Convergence Curve with Benchmark Function.

From the simulation results, the CSHO algorithm shows a good indication of the performance of the balance between the global and local search phases for optimization problems. In addition, the CSHO algorithm is also compared with the original SHO algorithm. The average convergence value of CSHO is lower than SHO

B. Comparison Trasient Response with Various Algorithm

The source of frequency and voltage constant in both angle and magnitude is an infinite bus. The Heffron-Philips model is used as a mathematical analysis for small signal stability analysis. The CSHO algorithm is applied with the aim of solving the non-linear optimization problem in obtaining the PSS parameter set. The expected parameters are expected to reduce wave oscillations optimally. The results of applying the CSHO algorithm to lead-lag PSS were compared with conventional PSS models, GOA, WOA and original SHO in two case studies.

In case study 1, the system is given a load of 100%. PSS parameters that have been obtained using the CSHO algorithm were tested with 100% load. In addition, PSS with the CSHO algorithm is compared with other approaches and the results can be seen in Fig. 4. Table V is the PSS parameters of each approach. The graph of case study 1 is presented in Fig. 4

In case study 1, the CSHO algorithm applied to PSS (PSS-CSHO) is able to reduce the overshoot and undershoot of the speed and rotor angle optimally. Comparison with the conventional PSS method (PSS-Conv), it is found that the PSS-CSHO algorithm is able to reduce overshoot by 6.79% for rotor angle and 7.25% for speed. Meanwhile, PSS-CSHO was able to reduce undershoot by 75.86% for angle and 5.96% for speed. Details of case study 1 are detailed in Table VI.

Comparison with PSS-WOA on the overshoot of the rotor angle, it was found that the PSS-WOA overshoot value was 47% better. Compared to PSS-CSHO. On the other hand, PSS-CSHO has a better speed overshoot of 61.87% compared to PSS-WOA.

TABLE V. THE RESULT OF PARAMETER PSS

Algorithm	Kpss	T1	T2	T3	T4
PSS-CSHO	-166.92626	266.7264	146.11179	1.7443	104.8790
PSS-SHO	23.7725	238.2281	-191.7066	2.433	24.1114
PSS-GOA	-64.7484	3.2133	100	-100	99.98
PSS-WOA	-38.5627	100	100	11.4185	100

TABLE VI. THE RESULT OF CASE STUDY 1

Algorithm	Rotor Angle Output				Speed Output		
	Overshoot	Undershoot	Rise Time (s)	Settling Time(s)	Overshoot	Undershoot	Settling Time(s)
PSS-CSHO	0.0208	-0.3658	426	1516	0.0098	-0.1051	673
PSS-SHO	0.0391	-0.4957	1375	1827	0.0113	-0.1229	661
PSS-GOA	0.308	-0.55	188	980	0.0141	-0.1287	681
PSS-WOA	0.011	-0.7395	189	607	0.0257	-0.1359	543
PSS-Conv	0.0887	-1.1244	32	593	0.0823	-0.1647	602

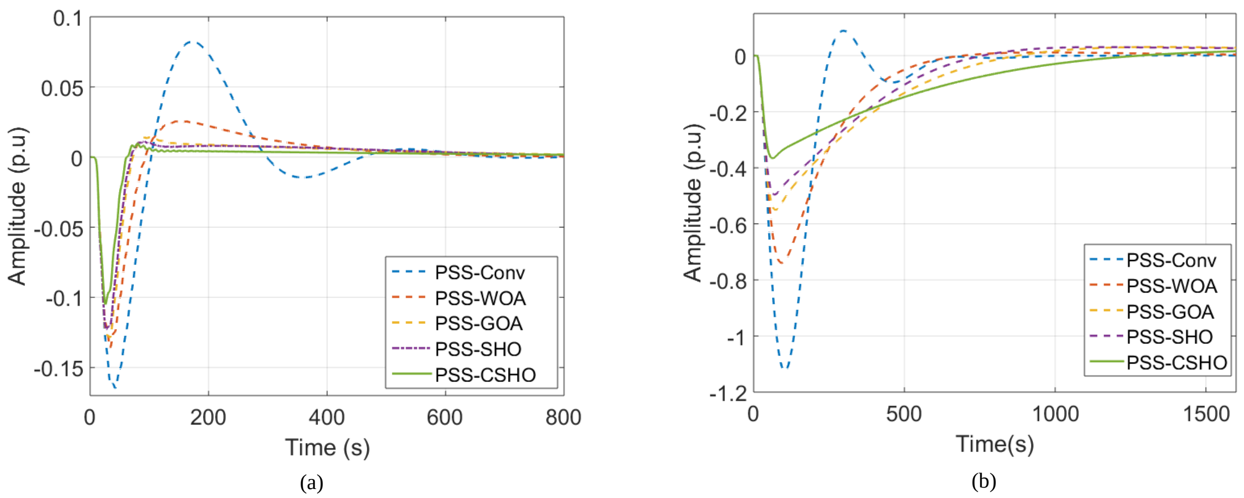

Fig. 4. Transient Response of Case Study 1 (a) Speed Response (b) Rotor Angle Response

TABLE VII. THE RESULT OF CASE STUDY 2

Algorithm	Rotor Output				Speed Output		
	Overshoot	Undershoot	Rise Time (s)	Settling Time(s)	Overshoot	Undershoot	Settling Time(s)
PSS-CSHO	0.0104	-0.1829	426	1517	0.0048	-0.0525	674
PSS-SHO	0.0195	-0.2478	1376	1827	0.0056	-0.0615	661
PSS-GOA	0.0154	-0.2750	188	980	0.0070	-0.0644	681
PSS-WOA	0.0056	-0.3697	1.758	607	0.0128	-0.0679	545
PSS-Conv	0.044	-0.5622	0.0025	487	0.0411	-0.0824	602

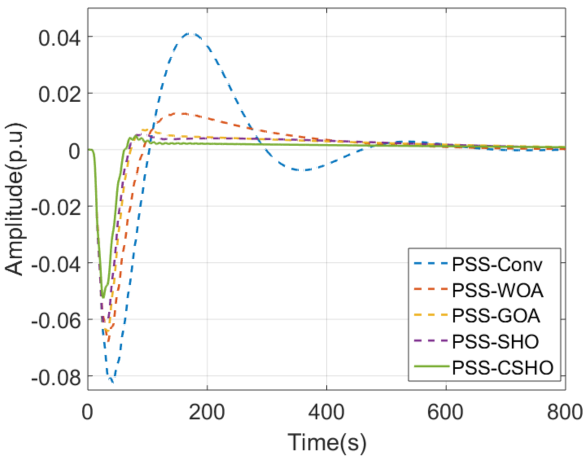

(a)

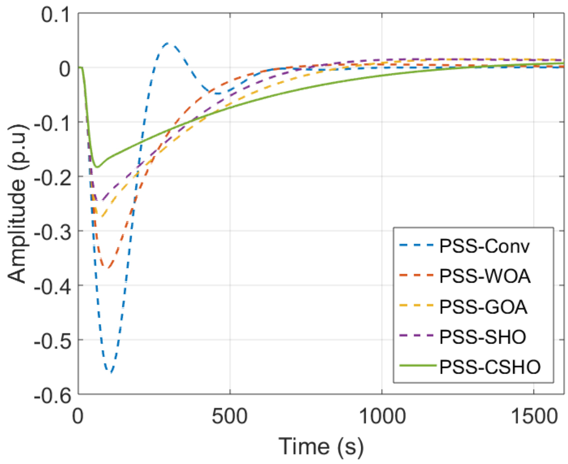

(b)

Fig. 5. Transient Response of Case Study 2 (a) Speed Response (b) Rotor Angle Response

The load is reduced by 50% in the case study 2. The response from case study 2 can be seen in detail in Table VII and the comparison graph can be seen in Fig. 5. PSS-CSHO has the optimal ability to reduce overshoot and undershoot in case study 2. Comparison with the method PSS-Conv found that the undershoot and overshoot of the PSS-CSHO method is better by 3.36% and 37.93% on the rotor angle. While on speed, PSS-CSHO method is 3.63% better on undershoot and 2.99% better on overshoot than PSS-Conv. On the rotor angle with PSS-WOA, a better overshoot value of 46.15% was obtained compared to PSS-CSHO. Meanwhile, at the speed with PSS-WOA, the overshoot value was worse than PSS-CSHO by 62.5%.

V. Conclusion and Future Works

In this article, the new improved SHO algorithm is a hybrid between the SHO method and the chaos map method. With this step, the SHO capability is improved. This method is called the CSHO method. CSHO is evaluated and validated with test functions and problems in the real world, namely in the power system. Testing begins by evaluating with the benchmark function. The results obtained were compared with WOA, GOA and SHO. The performance of CSHO shows a better improvement and shows a new balance point between exploration and exploitation. The next evaluation of the proposed CSHO is with real-world problems. In this article, CSHO is applied to obtain PSS parameters that can dampen oscillations optimally. The results obtained were compared with the conventional PSS method (PSS-Conv), PSS using WOA (PSS-WOA), PSS using GOA (PSS-GOA) and PSS using SHO (PSS-SHO). PSS using the CSHO algorithm has the ability to increase the transient stability of the SMIB system and optimal damping characteristics. From the two evaluation methods, it can be concluded that the implementation of the CSHO method shows an algorithm that has a strong approach to optimization problems.

This article uses integration with the chaotic method. This needs to be deepened into the concept of integration using methods that can sharpen the results of the convergence curve and conduct trials with more complex systems.

References

[1] G. Zhang *et al.*, "Deep reinforcement learning-based approach for proportional resonance power system stabilizer to prevent ultra-low-frequency oscillations," *IEEE Trans. Smart Grid*, vol. 11, no. 6, pp. 5260–5272, 2020, doi: 10.1109/TSG.2020.2997790.

[2] J. J. Kim and J. H. Park, "A novel structure of a power system stabilizer for microgrids," *Energies*, vol. 14, no. 4, p. 905, 2021, doi: 10.3390/en14040905.

[3] P. Sokólski, T. A. Rutkowski, B. Ceran, D. Horla, and D. Złotecka, "Power System Stabilizer as a Part of a Generator MPC Adaptive Predictive Control System," *Energies*, vol. 14, no. 20, p. 6631, 2021, doi: 10.3390/en14206631.

[4] F. Jamsheed and S. J. Iqbal, "A minimal architecture neuro adaptive predictive control scheme for power system stabilizer," *Int. J. Electr. Power Energy Syst.*, 2022, doi: 10.1016/j.ijepes.2021.107750.

[5] P. Marić, R. Kljajić, H. R. Chamorro, and H. Glavaš, "Power system stabilizer tuning algorithm in a multimachine system based on s-domain and time domain system performance measures," *Energies*, vol. 14, no. 18, p. 5644, 2021, doi: 10.3390/en14185644.

[6] J. Qi, Q. Wu, Y. Zhang, G. Weng, and D. Zhou, "Unified residue method for design of compact wide-area damping controller based on power system stabilizer," *J. Mod. Power Syst. Clean Energy*, vol. 8, no. 2, pp. 367–376, 2020, doi: 10.35833/MPCE.2018.000370.

[7] J. A. O. Lala and C. F. Gallardo, "Adaptive tuning of power system stabilizer using a damping control strategy considering stochastic time delay," *IEEE Access*, vol. 8, pp. 124254–124264, 2020, doi: 10.1109/ACCESS.2020.3004067.

[8] A. A. Canabal, A. G. Loukianov, J. M. C. Castañeda, and V. A. Utkin, "Adaptive power system stabilizer with sliding mode for electric power systems," *Int. J. Electr. Power Energy Syst.*, vol. 145, p. 108700, 2023, doi: 10.1016/j.ijepes.2022.108700.

[9] I. Davut, "A novel modified arithmetic optimization algorithm for power system stabilizer design," *Sigma J. Eng. Nat. Sci.*, vol. 40, no. 3, pp. 529–541, 2022, doi: 10.14744/sigma.2022.00056.

[10] D. Acharya and D. K. Das, "An Optimizer to Tune Fractional-Order Power System Stabilizer for Synchronous Generator Considering Governor Effect and Exciter Voltage Fluctuation," *J. Control. Autom. Electr. Syst.*, pp. 1–13, 2022, doi:10.1007/s40313-022-00962-7.

[11] M. Dehghani, M. Rezaei, B. Shayanfard, N. Vafamand, M. Javadi, and J. P. S. Catalão, "PMU-based power system stabilizer design: Optimal signal selection and controller design," *IEEE Trans. Ind. Appl.*, vol. 57, no. 6, pp. 5677–5686, 2021, doi: 10.1109/TIA.2021.3109572.

[12] A. A. El-Soud, S. H. Elbanna, and W. Sabry, "A strong action power system stabilizer employment to improve large scale power systems' stability," *J. Electr. Syst.*, vol. 17, no. 3, pp. 288–297, 2021.

[13] X. Zhou, M. Usman, P. He, M. S. Mastoi, and S. Liu, "Parameter design of governor power system stabilizer to suppress ultra-low-frequency oscillations based on phase compensation," *Electr. Eng.*,

vol. 103, no. 1, pp. 685–696, 2021, doi: 10.1007/s00202-020-01101-8.

[14] J. Huang, J. Liu, C. Zhang, Y. Kuang, and S. Weng, “Application of Improved Quasi-Affine Transformation Evolutionary Algorithm in Power System Stabilizer Optimization,” *Electronics*, vol. 11, no. 17, p. 2785, 2022, doi: 10.3390/electronics11172785.

[15] T. F. Do Nascimento and A. O. Salazar, “Power System Stabilizer Applied to VSG-Based Power Flow Control of DG Systems in Low-Voltage Networks,” in *2022 14th Seminar on Power Electronics and Control (SEPOC)*, 2022, pp. 1–6, doi: 10.1109/SEPOC54972.2022.9976432.

[16] A. Faraji, A. H. Naghshbandy, and A. G. Baayeh, “A Hybrid Coordinated Design Method for Power System Stabilizer and FACTS Device Based on Synchrosqueezed Wavelet Transform and Stochastic Subspace Identification,” *J. Mod. Power Syst. Clean Energy*, vol. 9, no. 4, pp. 910–918, 2020, doi: 10.35833/MPCE.2019.000496.

[17] K. M. Sreedivya, P. A. Jeyanthy, and D. Devaraj, “Improved design of interval type-2 fuzzy based wide area power system stabilizer for inter-area oscillation damping,” *Microprocess. Microsyst.*, vol. 83, p. 103957, 2021, doi: 10.1016/j.micpro.2021.103957.

[18] S. Essallah, A. Bouallegue, and A. Khedher, “Integration of automatic voltage regulator and power system stabilizer: small-signal stability in DFIG-based wind farms,” *J. Mod. Power Syst. Clean Energy*, vol. 7, no. 5, pp. 1115–1128, 2019, doi: 10.1007/s40565-019-0539-0.

[19] L. Swarupa, S. Lakshmi, O. Rubanenko, and D. Danylchenko, “Modeling, Simulation and Simultaneous Tuning Employing Genetic Algorithm in Power System With Power System Stabilizer with TCSC Controller,” in *2022 IEEE 3rd KhPI Week on Advanced Technology (KhPIWeek)*, 2022, pp. 1–5, doi: 10.1109/KhPIWeek57572.2022.9916504.

[20] G. M. Giannuzzi, D. Lauria, C. Pisani, and S. Tessitore, “An optimization procedure for power system stabilizer tuning,” in *2022 International Symposium on Power Electronics, Electrical Drives, Automation and Motion (SPEEDAM)*, 2022, pp. 112–117, doi: 10.1109/SPEEDAM53979.2022.9842034.

[21] R. M. A. Velásquez, T. T. P. Ezcurra, and L. F. V. Aldon, “Power System Stabilizer Design with meta-heuristic methods in a Peruvian case study,” in *2022 IEEE XXIX International Conference on Electronics, Electrical Engineering and Computing (INTERCON)*, 2022, pp. 1–4, doi: 10.1109/INTERCON55795.2022.9870161.

[22] R. Hemmati, “Power system stabilizer design based on optimal model reference adaptive system,” *Ain Shams Eng. J.*, vol. 9, no. 2, pp. 311–318, 2018, doi: 10.1016/j.asej.2016.03.002.

[23] K. Eltag, M. S. Aslamx, and R. Ullah, “Dynamic stability enhancement using fuzzy PID control technology for power system,” *Int. J. Control. Autom. Syst.*, vol. 17, no. 1, pp. 234–242, 2019, doi: 10.1007/s12555-018-0109-7.

[24] P. Chaubey, J. S. Lather, S. Yelisetti, S. Manda, and N. K. Yadav, “Robust power system stabilizer based on static output feedback approach to enhance power system stability,” *Energy Procedia*, vol. 158, pp. 2960–2965, 2019, doi: 10.1016/j.egypro.2019.01.959.

[25] B. Douidi, L. Mokrani, and M. Machmoum, “A new cascade fuzzy power system stabilizer for multi-machine system stability enhancement,” *J. Control. Autom. Electr. Syst.*, vol. 30, no. 5, pp. 765–779, 2019, doi: 10.1007/s40313-019-00486-7.

[26] M. A. Prakasa and I. Robandi, “Power System Stabilizer Tuning Improvement for Single-Machine Infinite Bus using Equilibrium Optimizer Algorithm,” in *2022 International Seminar on Intelligent Technology and Its Applications (ISITIA)*, 2022, pp. 320–325, doi: 10.1109/ISITIA56226.2022.9855203.

[27] P. Kibet, H. A. Ouma, and P. M. Moses, “Improvement of Small Signal Stability by Tuning Power System Stabilizer Parameters for Geothermal Generation,” in *2022 IEEE PES/IAS PowerAfrica*, 2022, pp. 1–5, doi: 10.1109/PowerAfrica53997.2022.9905319.

[28] W. Hu, J. Liang, Y. Jin, and F. Wu, “Model of power system stabilizer adapting to multi-operating conditions of local power grid and parameter tuning,” *Sustainability*, vol. 10, no. 6, p. 2089, 2018, doi: 10.3390/su10062089.

[29] X. Li, J. Fu, X. Zhang, H. Cao, Z. Lin, and Y. Niu, “A neural power system stabilizer of DFIGs for power system stability support,” *Int. Trans. Electr. Energy Syst.*, vol. 28, no. 6, p. e2547, 2018, doi: 10.1002/etep.2547.

[30] A. Salgotra and S. Pan, “Model based PI power system stabilizer design for damping low frequency oscillations in power systems,” *ISA Trans.*, vol. 76, pp. 110–121, 2018, doi: 10.1016/j.isatra.2018.03.013.

[31] S. Tusun, I. Erceg, M. Mehmedović, and D. Sumina, “Decentralized synergetic power system stabilizer,” *Electr. Eng.*, vol. 100, no. 1, pp. 311–320, 2018, doi: 10.1007/s00202-016-0506-y.

[32] A. Hadap and S. Vaishnav, “H-robust technique based ant optimal power system for solar energy power system stabilizer,” *Materials Today: Proceedings*, vol. 51, pp. 118-124, 2022, doi: 10.1016/j.matpr.2021.04.602.

[33] J. Shen *et al.*, “Small signal stability analysis of isolated power system with different load types and power system stabilizer,” *11th International Conference on Renewable Power Generation - Meeting net zero carbon (RPG 2022)*, 2022, pp. 85-89, doi: 10.1049/icp.2022.1676.

[34] B. M. Alshammari, A. Farah, K. Alqunun, and T. Guesmi, “Robust Design of Dual-Input Power System Stabilizer Using Chaotic JAYA Algorithm,” *Energies*, vol. 14, no. 17, p. 5294, 2021, doi: 10.3390/en14175294.

[35] I. M. Alotaibi, S. Ibrir, M. A. Abido, and M. Khalid, “Nonlinear Power System Stabilizer Design for Small Signal Stability Enhancement,” *Arab. J. Sci. Eng.*, pp. 1–13, 2022, doi: 10.1007/s13369-022-06566-2.

[36] A. Sabo, N. I. Abdul Wahab, M. L. Othman, M. Z. A. Mohd Jaffar, and H. Beiranvand, “Optimal design of power system stabilizer for multimachine power system using farmland fertility algorithm,” *Int. Trans. Electr. Energy Syst.*, vol. 30, no. 12, p. e12657, 2020, doi: 10.1002/2050-7038.12657.

[37] H. Mohammed and T. Rashid, “FOX: a FOX-inspired optimization algorithm,” *Appl. Intell.*, pp. 1–21, 2022, doi: 10.1007/s10489-022-03533-0.

[38] H. T. Sadeeq and A. M. Abdulazeez, “Giant Trevally Optimizer (GTO): A Novel Metaheuristic Algorithm for Global Optimization and Challenging Engineering Problems,” *IEEE Access*, vol. 10, pp. 121615–121640, 2022, doi: 10.1109/ACCESS.2022.3223388.

[39] J. Xue and B. Shen, “Dung beetle optimizer: a new meta-heuristic algorithm for global optimization,” *J. Supercomput.*, pp. 1–32, 2022, doi: 10.1007/s11227-022-04959-6.

[40] O. N. Oyelade, A. E. S. Ezugwu, T. I. A. Mohamed, and L. Abualigah, “Ebola Optimization Search Algorithm: A New Nature-Inspired Metaheuristic Optimization Algorithm,” *IEEE Access*, 2022, doi: 10.1109/ACCESS.2022.3147821.

[41] J. O. Agushaka, A. E. Ezugwu, and L. Abualigah, “Dwarf Mongoose Optimization Algorithm,” *Comput. Methods Appl. Mech. Eng.*, 2022, doi: 10.1016/j.cma.2022.114570.

[42] F. A. Hashim and A. G. Hussien, “Snake Optimizer: A novel meta-heuristic optimization algorithm,” *Knowledge-Based Syst.*, 2022, doi: 10.1016/j.knosys.2022.108320.

[43] L. Abualigah, A. Diabat, S. Mirjalili, M. Abd Elaziz, and A. H. Gandomi, “The arithmetic optimization algorithm,” *Comput. Methods Appl. Mech. Eng.*, vol. 376, p. 113609, 2021, doi: 10.1016/j.cma.2020.113609.

[44] F. A. Hashim, K. Hussain, E. H. Houssein, M. S. Mabrouk, and W. Al-Atabany, “Archimedes optimization algorithm: a new metaheuristic algorithm for solving optimization problems,” *Appl. Intell.*, vol. 51, no. 3, pp. 1531–1551, 2021, doi: 10.1007/s10489-020-01893-z.

[45] H. Jia, X. Peng, and C. Lang, “Remora optimization algorithm,” *Expert Syst. Appl.*, vol. 185, p. 115665, 2021, doi: 10.1016/j.eswa.2021.115665.

[46] B. Abdollahzadeh, F. S. Gharehchopogh, and S. Mirjalili, “African vultures optimization algorithm: A new nature-inspired metaheuristic algorithm for global optimization problems,” *Comput. Ind. Eng.*, vol. 158, p. 107408, 2021, doi: 10.1016/j.cie.2021.107408.

[47] F. MiarNaeimi, G. Azizyan, and M. Rashki, “Horse herd optimization algorithm: a nature-inspired algorithm for high-dimensional optimization problems,” *Knowledge-Based Syst.*, vol. 213, p. 106711, 2021, doi: 10.1016/j.knosys.2020.106711.

[48] T. Rahkar Farshi, “Battle royale optimization algorithm,” *Neural Comput. Appl.*, vol. 33, no. 4, pp. 1139–1157, 2021, doi: 10.1007/s00521-020-05004-4.

[49] M. Khishe and M. R. Mosavi, “Chimp optimization algorithm,” *Expert Syst. Appl.*, vol. 149, p. 113338, 2020, doi:

10.1016/j.eswa.2020.113338.

[50] P. Trojovský and M. Dehghani, "Pelican optimization algorithm: A novel nature-inspired algorithm for engineering applications," *Sensors*, vol. 22, no. 3, p. 855, 2022, doi: 10.3390/s22030855.

[51] A. E. Ezugwu, J. O. Agushaka, L. Abualigah, S. Mirjalili, and A. H. Gandomi, "Prairie dog optimization algorithm," *Neural Comput. Appl.*, pp. 1–49, 2022, doi: 10.3390/s22030855.

[52] L. Abualigah, "Group search optimizer: a nature-inspired meta-heuristic optimization algorithm with its results, variants, and applications," *Neural Comput. Appl.*, vol. 33, no. 7, pp. 2949–2972, 2021, doi: 10.1007/s00521-020-05107-y.

[53] D. Izci, "A novel improved atom search optimization algorithm for designing power system stabilizer," *Evol. Intell.*, vol. 15, no. 3, pp. 2089–2103, 2022, doi: 10.1007/s12065-021-00615-9.

[54] H. Setiadi, F. Arrazi, M. Abdillah, and A. U. Krismanto, "Smart DIPSS for Dynamic Stability Enchancement on Multi-Machine Power System," *Indones. J. Electr. Eng. Informatics*, vol. 10, no. 1, pp. 43–50, 2022, doi: 10.52549/ijeei.v10i1.3429.

[55] M. A. Kamarposhti, I. Colak, C. Iwendi, S. S. Band, and E. Ibeke, "Optimal coordination of PSS and SSSC controllers in power system using ant colony optimization algorithm," *J. circuits, Syst. Comput.*, vol. 31, no. 04, p. 2250060, 2022, doi: 10.1142/S0218126622500608.

[56] H. Yokus and A. Ozturk, "A robust crow search algorithm-based power system stabilizer for the SMIB system," *Neural Comput. Appl.*, vol. 34, no. 11, pp. 9161–9173, 2022, doi: 10.1007/s00521-022-06943-w.

[57] J. H. Tayeb, M. R. Islam, M. Shafiullah, S. M. A. Gani, and M. I. Hossain, "Robust Power System Stabilizer for Multi-machine Power Networks using Tunicate Swarm Algorithm," in *2022 Second International Conference on Artificial Intelligence and Smart Energy (ICAIS)*, 2022, pp. 1761–1766, doi: 10.1109/ICAIS53314.2022.9741828.

[58] L. Chaib, A. Choucha, S. Arif, H. G. Zaini, A. El-Fergany, and S. S. M. Ghoneim, "Robust design of power system stabilizers using improved harris hawk optimizer for interconnected power system," *Sustainability*, vol. 13, no. 21, p. 11776, 2021, doi: 10.3390/su132111776.

[59] S. R. Paital, P. K. Ray, and S. R. Mohanty, "A robust dual interval type-2 fuzzy lead–lag based upfc for stability enhancement using harris hawks optimization," *ISA Trans.*, vol. 123, pp. 425–442, 2022, doi: 10.1016/j.isatra.2021.05.029.

[60] N. Razmjooy, S. Razmjooy, Z. Vahedi, V. V Estrela, and G. G. de Oliveira, "A new design for robust control of power system stabilizer based on Moth search algorithm," in *Metaheuristics and Optimization in Computer and Electrical Engineering*, pp. 187–202, 2021, doi: 10.1007/978-3-030-56689-0_10 .

[61] D. K. Lal and A. K. Barisal, "Combined load frequency and terminal voltage control of power systems using moth flame optimization algorithm," *J. Electr. Syst. Inf. Technol.*, vol. 6, no. 1, pp. 1–24, 2019, doi: 10.1186/s43067-019-0010-3.

[62] E. V Fortes, L. F. B. Martins, M. V. S. Costa, L. Carvalho, L. H. Macedo, and R. Romero, "Mayfly Optimization Algorithm Applied to the Design of PSS and SSSC-POD Controllers for Damping Low-Frequency Oscillations in Power Systems," *Int. Trans. Electr. Energy Syst.*, vol. 2022, 2022, doi: 10.1155/2022/5612334.

[63] R. Devarapalli and B. Bhattacharyya, "Optimal controller parameter tuning of PSS using sine-cosine algorithm," in *Metaheuristic and Evolutionary Computation: Algorithms and Applications*, pp. 337–360, 2021, doi: 10.1007/978-981-15-7571-6_15.

[64] A. Toolabi Moghadam, M. Aghahadi, M. Eslami, S. Rashidi, B. Arandian, and S. Nikolovski, "Adaptive Rat Swarm Optimization for Optimum Tuning of SVC and PSS in a Power System," *Int. Trans. Electr. Energy Syst.*, vol. 2022, 2022, doi: 10.1155/2022/4798029.

[65] P. R. Sahu, P. K. Hota, and S. Panda, "Modified whale optimization algorithm for coordinated design of fuzzy lead-lag structure-based SSSC controller and power system stabilizer," *Int. Trans. Electr. Energy Syst.*, vol. 29, no. 4, p. e2797, 2019, doi: 10.1002/etep.2797.

[66] B. Dasu, M. Sivakumar, and R. Srinivasarao, "Interconnected multi-machine power system stabilizer design using whale optimization algorithm," *Prot. Control Mod. Power Syst.*, vol. 4, no. 1, pp. 1–11, 2019, doi: 10.1186/s41601-019-0116-6.

[67] D. Wang, N. Ma, M. Wei, and Y. Liu, "Parameters tuning of power system stabilizer PSS4B using hybrid particle swarm optimization algorithm," *Int. Trans. Electr. Energy Syst.*, vol. 28, no. 9, p. e2598, 2018, doi: 10.1002/etep.2598.

[68] T. H. Elmenfy, "Design of Velocity PID-Fuzzy Power System Stabilizer Using Particle Swarm Optimization," *WSEAS Trans. Syst.*, vol. 20, pp. 9–14, 2021, doi: 10.37394/23202.2021.20.2.

[69] S. Latif, S. Irshad, M. Ahmadi Kamarposhti, H. Shokouhandeh, I. Colak, and K. Eguchi, "Intelligent Design of Multi-Machine Power System Stabilizers (PSSs) Using Improved Particle Swarm Optimization," *Electronics*, vol. 11, no. 6, p. 946, 2022, doi: 10.3390/electronics11060946.

[70] S. K. Mony, A. J. Peter, and D. Durairaj, "Gaussian quantum particle swarm optimization-based wide-area power system stabilizer for damping inter-area oscillations," *World J. Eng.*, 2021, doi: 10.1108/WJE-05-2021-0303.

[71] M. K. Gude and U. Salma, "A novel approach of PSS optimal parameter tuning in a multi-area power system using hybrid butterfly optimization algorithm-particle swarm optimization," *Int. J. Syst. Assur. Eng. Manag.*, pp. 1–10, 2022, doi: 10.1007/s13198-022-01678-2.

[72] K. Kalegowda, A. D. I. Srinivasan, and N. Chinnamadha, "Particle swarm optimization and Taguchi algorithm-based power system stabilizer-effect of light loading condition.," *Int. J. Electr. Comput. Eng.*, vol. 12, no. 5, 2022, doi: 10.11591/ijece.v12i5.pp4672-4679.

[73] R. Devarapalli, B. Bhattacharyya, and N. K. Sinha, "An intelligent EGWO-SCA-CS algorithm for PSS parameter tuning under system uncertainties," *Int. J. Intell. Syst.*, vol. 35, no. 10, pp. 1520–1569, 2020, doi: 10.1002/int.22263.

[74] G. Penchalaiah and R. Ramya, "Stability enhancement of power system based on HHO-TSA control scheme," *Int. J. Electron.*, pp. 1–27, 2021, doi: 10.1080/00207217.2021.2001871.

[75] S. Zhao, T. Zhang, S. Ma, and M. Wang, "Sea-horse optimizer: a novel nature-inspired meta-heuristic for global optimization problems," *Appl. Intell.*, pp. 1–28, 2022, doi: 10.1007/s10489-022-03994-3.

[76] B. Hekimoğlu, "Optimal tuning of fractional order PID controller for DC motor speed control via chaotic atom search optimization algorithm," *IEEE Access*, vol. 7, pp. 38100–38114, 2019, doi: 10.1109/ACCESS.2019.2905961.

[77] A. Rodríguez-Molina, M. G. Villarreal-Cervantes, O. Serrano-Pérez, J. Solís-Romero, and R. Silva-Ortigoza, "Optimal Tuning of the Speed Control for Brushless DC Motor Based on Chaotic Online Differential Evolution," *Mathematics*, vol. 10, no. 12, p. 1977, 2022, doi: 10.3390/math10121977.

[78] E. S. Bayu, B. Khan, Z. M. Ali, Z. M. Alaas, and O. P. Mahela, "Mitigation of Low-Frequency Oscillation in Power Systems through Optimal Design of Power System Stabilizer Employing ALO," *Energies*, vol. 15, no. 10, p. 3809, 2022, doi: 10.3390/en15103809.

[79] W. Aribowo, S. Muslim, B. Suprianto, S. Haryudo, and A. C. Hermawan, "Intelligent Control of Power System Stabilizer Based on Archimedes Optimization Algorithm–Feed Forward Neural Network," *Int. J. Intell. Eng. Syst.*, vol. 14, no. 3, pp. 43–53, 2021, doi: 10.22266/ijies2021.0630.05.

[80] N. Azizi, H. Moradi CheshmehBeigi, and K. Rouzbehi, "HVDC grids stability improvement by direct current power system stabilizer," *IET Gener. Transm. Distrib.*, vol. 16, no. 3, pp. 492–502, 2022, doi: 10.1049/gtd2.12295.

[81] W. Aribowo, S. Muslim, B. Suprianto, and S. I. H. Joko, "Tunicate swarm algorithm-neural network for adaptive power system stabilizer parameter," *Sci. Technol. Asia*, vol. 26, no. 3, pp. 50–63, 2021, doi: 10.14456/scitechasia.2021.46.

[82] L. Xie, T. Han, H. Zhou, Z.-R. Zhang, B. Han, and A. Tang, "Tuna swarm optimization: a novel swarm-based metaheuristic algorithm for global optimization," *Comput. Intell. Neurosci.*, vol. 2021, 2021, doi: 10.1155/2021/9210050.

[83] T. S. L. V Ayyarao *et al.*, "War strategy optimization algorithm: a new effective metaheuristic algorithm for global optimization," *IEEE Access*, vol. 10, pp. 25073–25105, 2022, doi: 10.1109/ACCESS.2022.3153493.